

Article

Theoretical Structure and Applications of a Newly Enhanced Gumbel Type II Model

Showkat Ahmad Lone ¹, Tabassum Naz Sindhu ^{2,*}, Marwa K. H. Hassan ³, Tahani A. Abushal ^{4,*},
Sadia Anwar ⁵ and Anum Shafiq ^{6,7,*}

- ¹ Department of Basic Sciences, College of Science and Theoretical Studies, Saudi Electronic University, Riyadh 11673, Saudi Arabia
 - ² Department of Statistics, Quaid-i-Azam University, Islamabad 44000, Pakistan
 - ³ Department of Mathematics, Faculty of Education, Ain Shams University, Cairo 11566, Egypt
 - ⁴ Department of Mathematical Science, Faculty of Applied Science, Umm Al-Qura University, Makkah 24382, Saudi Arabia
 - ⁵ Department of Mathematics, College of Arts and Sciences, Wadi Ad Dawasir, Prince Sattam Bin Abdul Aziz University, Al-Kharj 11991, Saudi Arabia
 - ⁶ School of Mathematics and Statistics, Nanjing University of Information Science and Technology, Nanjing 210044, China
 - ⁷ Jiangsu International Joint Laboratory on System Modeling and Data Analysis, Nanjing University of Information Science and Technology, Nanjing 210044, China
- * Correspondence: sindhuqu@gmail.com (T.N.S.); taabushal@uqu.edu.sa (T.A.A.); anumshafiq@ymail.com or anum_shafiq@nuist.edu.cn (A.S.)

Abstract: Statistical models are vital in data analysis, and researchers are always on the search for potential or the latest statistical models to fit data sets in a variety of domains. To create an improved statistical model, we used a T-X transformation and the Gumbel Type-II model in this investigation. The research examined a simulation evaluation to assess the efficacy of the parameters. To show the application of the T-X approach for producing new distributions titled the new and improved Gumbel Type-II (NIGT-II) distribution, two actual data sets were used. The data sets reveal that the NIGT-II distribution sounds nicer than the Gumbel Type-II distribution.



Citation: Lone, S.A.; Sindhu, T.N.; Hassan, M.K.H.; Abushal, T.A.; Anwar, S.; Shafiq, A. Theoretical Structure and Applications of a Newly Enhanced Gumbel Type II Model. *Mathematics* **2023**, *11*, 1797. <https://doi.org/10.3390/math11081797>

Academic Editor: Alicia Nieto-Reyes

Received: 22 February 2023

Revised: 22 March 2023

Accepted: 3 April 2023

Published: 10 April 2023



Copyright: © 2023 by the authors. Licensee MDPI, Basel, Switzerland. This article is an open access article distributed under the terms and conditions of the Creative Commons Attribution (CC BY) license (<https://creativecommons.org/licenses/by/4.0/>).

Keywords: mean square error; T-X method; root mean square error; NIGT-II model; average bias

MSC: 60E05; 62E15

1. Introduction

When making decisions under uncertainty, probability distribution is very important. Its applications include signal processing, survival analysis, and reliability analysis, and also communication systems and engineering. It has been observed in the field of probability theory that typical probability models lack to describe data with non-monotonic hazard functions (NMNHF) [1,2]. For instance, the Weibull model [3] cannot interpret data with a non-monotonic bath-tub hazard structure. To simulate the monotonic hazard rate, we can implement the Gamma, Gumbel type-II (GT-II), Weibull and exponential distributions, among other existing models. In the event of NMNHF, such as upside-down or bathtub-formed hazard rates, such models are neither rational nor practicable. In actuality, there are various data sets that have a non-monotonic failure rate function (FRF). To simulate both monotonic (MN) and NMHFs, one must update the existing distribution. In order to tackle this challenge, researchers are working to improve existing models. Both raising the number of factors in the benchmark model and developing a novel strategy for expanding probability models are necessary enhancements.

The idea of creating novel models by adding an additional element to a presenting group of models or mixing existing models has been a popular topic in recent studies. It

enables a more adjustable model while also allowing for the modeling of more complex data structures. Yet, the most recent modification has indicated that more characteristics are required to properly understand the tails and other elements of the distribution. Applied statisticians can now obtain better results by following the latest trend, as the extended model has a higher goodness of fit to data sets than the traditional method. After proposing the beta generator [4,5], the invention commences. Later on, several potential generators including the Kumaraswamy-G by [6] and the McDonald-G by [7] are presented. Comparing the effectiveness of some probability models to that of other G-class models was equally enjoyable for experts and applied investigators. Similar studies have been reported using G-classes of distributions: Exponentiated-Generalized-G [8], Gamma-G (type 1 and 2) [9], Lomax-G [10], Logistic-X [11], Weibull-G (type 3) [12], Odd Generalized-Exponential-G [13], Weibull-G (type 1) [14], and Fréchet Topp Leone-G [15].

In the literature, there are numerous methods for making the model wider and more adaptive in order to model the data. For illustration, Aldeni et al. [16] proposed a novel group of models centered on the quantile of the generalized lambda model. Alzaatreh et al. [17] looked into T-normal family of models. Cordeiro et al. [18] studied a half-Cauchy group of models that can be applied to real-world phenomena. Ref. [19] modified [20]'s technique by replacing the Kumaraswamy model for the beta distribution. Alpha Power Transformation (APT), which was proposed in [21], is another method. The two-parameter Alpha Power Exponential (APE) model, which has a number of properties and ramifications, was generated using the APT technique. Many expansions of the APT techniques to modeling Weibull models have lately been tried by researchers [22,23]. Several investigators have utilized this transformation to generate alpha power transformed models using an APT generalized exponential model, APT inverse Lindley model [24], and APT Lindley model [25]. Ijaz et al. [26] provided the Gull Alpha Power family of models (GAPF).

Extreme value models have grown in popularity as a statistical research subject in a variety of fields. Extreme point strategies are increasing in interest in a number of different zones as well. The probability of incidents that are more serious than those earlier recorded must sometimes be calculated in extreme point investigations. The Gumbel model is a valuable model in extreme value theory. It has a vast storage potential that can be used in the event of a major calamity. Life testing, fracture roughness, seismology, reliability analysis, and meteorology are only a few examples of applications for such models. Tables of life expectancy, hydrology, and rainfall can also be used. Detailed descriptions of the Gumbel distribution can be found in [27–31]. It can be utilized to represent real-world data sets with monotonic failure rates, especially those with declining hazard rates. However, the majority of complex events are non-monotonic, and the Gumbel type-II (GT-II) model cannot be used to model them.

Alzaatreh [32] and Alzaatreh et al. [33] characterized the transformed (T)-transformer (X) family (for brief, T-X family), which marked a turning point in the G-class paradigm. This study centers on the T-X family of probability models (see Alzaatreh et al. [32]), and leverages GT-II models' CDF to create a generalized form referred to as the new and improved GT-II (NIGT-II) distribution. Since it can provide a broad variety of shapes for the hazard function, the NIGT-II model has a lot of versatility and will play a big part in medical and reliability investigations. We believe that NIGT-II will attract a greater range of applications and will be used to represent a variety of data types in a variety of fields. We have identified several statistical characteristics and shown how to apply the proposed probability function to both actual and simulated data. When examining any probability model, parameter estimation is essential. We employ the maximum likelihood estimation (MaxLLE) approach to evaluate the model's undetermined parameters. References [34–43] contain more examples of estimation of the model's undetermined parameters.

2. Description of Proposed Model

Let $\pi(t)$ be a PDF of T such that $T \in [\eta, m]$ for $-\infty \leq \eta < m \leq \infty$, and $W\{G(x)\}$ be a function of CDF $G(x)$ with PDF $f(x)$ of any r.v. X that $W\{G(x)\}$ fulfils given criteria: (i) $W\{G(x)\} \in [\eta, m]$, (ii) $W\{G(x)\}$ must be able to be differentiated and non-decreasing monotonically and (iii) $W\{G(x)\} \rightarrow \eta$ as $t \rightarrow -\infty$ and $W\{G(x)\} \rightarrow m$ as $t \rightarrow \infty$. Then, the CDF of a T-X family (see [32]) of models is characterized by expression (1)

$$F(x) = \int_{\eta}^{W\{G(x)\}} \pi(t) dt, \tag{1}$$

The CDF $F(x)$ in (1) can be $P[W\{G(x)\}]$, where $P(t)$ is the CDF of T . The PDF refers to (1) given by expression (2)

$$f(x) = \frac{dW\{G(x)\}}{dx} \pi(W\{G(x)\}). \tag{2}$$

Because of its usefulness, many scholars prefer to work with the T-X family methodology. Nonetheless, some new model families have been given in the literature; see [44] for more information. We suggest a novel family of models centered on the T family in this study. Let $T \sim exp(1)$, with CDF and PDF having the forms as below $P(t) = 1 - e^{-t}$, $\pi(t) = e^{-t}$, and letting

$$W\{G(x)\} = -\log\left\{\frac{1 - G(x)}{\lambda^{G(x)}}\right\} \tag{3}$$

in (1), we get a new CDF and PDF of the novel lifetime T-X family as follows:

$$F(x, \lambda) = 1 - \frac{1 - G(x)}{\lambda^{G(x)}}, \tag{4}$$

$$f(x) = g(x) \left\{ \frac{1 + (1 - G(x)) \log \lambda}{\lambda^{G(x)}} \right\} \tag{5}$$

The GT-II model's CDF and PDF are provided as follows.

$$G(x|\mu, \zeta) = e^{-\mu x^{-\zeta}}, \quad \mu, \zeta > 0, \text{ and } 0 < x < \infty, \tag{6}$$

$$g(x|\mu, \zeta) = \mu \zeta x^{-\zeta-1} e^{-\mu x^{-\zeta}}. \tag{7}$$

Let T be an r. v. such that $t > 0$, and the CDF and PDF of the NIGT-II lifespan model is stated as

$$F_{\text{NIGT-II}}(x|\mu, \zeta, \lambda) = 1 - \left(\frac{1 - e^{-\mu x^{-\zeta}}}{\lambda e^{-\mu x^{-\zeta}}} \right), \quad \mu, \zeta, \lambda > 0, \tag{8}$$

where μ is the scale and $\lambda, \zeta > 0$ are the shape parameters, accordingly. The GT-II model is a particular example if we consider $\lambda = 1$. The PDF for (8) is as follows:

$$f_{\text{NIGT-II}}(x|\mu, \zeta, \lambda) = \mu \zeta x^{-\zeta-1} e^{-\mu x^{-\zeta}} \left\{ \frac{1 + (1 - e^{-\mu x^{-\zeta}}) \log \lambda}{\lambda e^{-\mu x^{-\zeta}}} \right\}, \quad 0 < x < \infty, \mu, \zeta, \lambda > 0. \tag{9}$$

The phrase “failure rate function (FRF)” is frequently used in research. This phrase is used to describe the failure rate of an element over a particular time period (t) and is expressed as $h(t|.) = f(t|.)/[1 - F(t|.)]$. The FRF

$$h_{\text{NIGT-II}}(x|\mu, \zeta, \lambda) = \frac{\mu\zeta x^{-\zeta-1}e^{-\mu x^{-\zeta}} \left\{ 1 + (1 - e^{-\mu x^{-\zeta}}) \log \lambda \right\}}{1 - e^{-\mu x^{-\zeta}}}, \tag{10}$$

an excellent approach for studying reliability. The reliability function indicates the likelihood of an item surviving at time t . It is described analytically as $S(x|\mu, \zeta, \lambda) = 1 - F(x|\mu, \zeta, \lambda)$. Here, $S(x|\mu, \zeta, \lambda)$ of the NIGT-II model is

$$S_{\text{NIGT-II}}(x|\mu, \zeta, \lambda) = \left(\frac{1 - e^{-\mu x^{-\zeta}}}{\lambda e^{-\mu x^{-\zeta}}} \right). \tag{11}$$

The CHRF is one of the most important reliability metrics. The CHRF is a risk index: the larger $H(t|\mu, \zeta, \lambda)$, the greater the probability of t -time collapse.

$$H_{\text{NIGT-II}}(t|\mu, \zeta, \lambda) = \int_0^t h(x|\mu, \zeta, \lambda)dx = -\log[S(t|\mu, \zeta, \lambda)], \tag{12}$$

where $S(t|\mu, \zeta, \lambda)$ is given in (11), after replacing x by t , we have

$$H_{\text{NIGT-II}}(t|\mu, \zeta, \lambda) = -\log\left(\frac{1 - e^{-\mu t^{-\zeta}}}{\lambda e^{-\mu t^{-\zeta}}}\right). \tag{13}$$

The Mills ratio is defined by $M(x|\mu, \zeta, \lambda) = S(x|\mu, \zeta, \lambda)/f(x|\mu, \zeta, \lambda)$. A Mills ratio of X is

$$M_{\text{NIGT-II}}(x|\mu, \zeta, \lambda) = \frac{1 - e^{-\mu x^{-\zeta}}}{\mu\zeta x^{-\zeta-1}e^{-\mu x^{-\zeta}} \left\{ 1 + (1 - e^{-\mu x^{-\zeta}}) \log \lambda \right\}}. \tag{14}$$

The odd function is defined by $O(x|\mu, \zeta, \lambda) = F(x|\mu, \zeta, \lambda)/S(x|\mu, \zeta, \lambda)$. The odd function is

$$O_{\text{NIGT-II}}(x|\mu, \zeta, \lambda) = \frac{\lambda e^{-\mu x^{-\zeta}}}{1 - e^{-\mu x^{-\zeta}}} - 1. \tag{15}$$

The RHRF ($x|\mu, \zeta, \lambda$) (reverse hazard rate function) is defined by $RHRF(x|\mu, \zeta, \lambda) = f(x|\mu, \zeta, \lambda)/F(x|\mu, \zeta, \lambda)$. The RHRF of X is given by

$$RHRF_{\text{NIGT-II}}(x|\Psi) = \mu\zeta x^{-\zeta-1}e^{-\mu x^{-\zeta}} \left\{ \frac{1 + (1 - e^{-\mu x^{-\zeta}}) \log \lambda}{\lambda e^{-\mu x^{-\zeta}} + e^{-\mu x^{-\zeta}} - 1} \right\}. \tag{16}$$

Novelty and Innovation

The following are the primary contributions of this study’s innovative impact on the GT-II model utilizing the T-X approach:

- A simple and quick way for improving current distributions and simple technique to incorporate an extra parameters ‘ λ ’ to benchmark distribution.
- The T-X method improves and enriches the distribution.
- Using the T-X family to increase the features and versatility of the GT-II distribution (as motivated above). The probability density and hazard rate functions, in particular, exhibit growing, decreasing, bathtub, reverse J, increasing–decreasing and S shapes demonstrating this argument.
- Current distribution features and flexibility are being improved.
- The T-X method can be used to simulate both MN and NMNHF.

- We get a better fit with the T-X technique than with the GT-II model.
- Demonstrating a more advanced version of the GT-II model.
- Examining the inferential properties of the NIGT-II model using the MaxLLE, providing a comprehensive paradigm for users.

2.1. Shape

Based on various parameter values, Figure 1a–h depicts potential NIGT-II density shapes. The declining, bathtub, symmetric, asymmetric, and inverted J forms are among the many shapes of the PDF corresponding to μ , which controls the model’s scale, as well as the two shape parameters, ζ and λ which control the model’s shapes. Figure 1a–h illustrates instances of such structures. FRF patterns for the NIGT-II model are shown in Figure 2a–h. These figures demonstrate the FRF patterns, which comprise inverted J, bathtub, increasing–decreasing, and S patterns. These adjustable FRF forms are suitable for both MN and NMN failure rate characteristics, both of which are frequent in real-time applications. These types of forms are common in non-stationary lifespan events.

2.2. Simulation

The theory of a quantile function (QF) was first introduced by Hyndman and Fan [45]. Inverting the CDF (5) yields the QF of the NIGT-II model. Let ω be a variable such that $\omega \sim U(0, 1)$. A solution of a nonlinear equation can be used to provide an observation of X .

$$x(\omega | \mu, \zeta, \lambda) = \mu x^{-\zeta} + \log \left\{ 1 - \lambda e^{-\mu x^{-\zeta}} (1 - \omega) \right\}, \quad 0 < \omega < 1. \tag{17}$$

Computational strategies such as Newton–Raphson techniques can be engaged to estimate X from (17). The median of the NIGT-II model is presented here. Let $F(x|.)$ be the CDF of NIGT-II model at 0.5th quantile $Q_{0.5}$. The median (x^*) can therefore be given by solving the given equation for x .

$$\mu x^{-\zeta} + \log \left\{ 1 - 0.5\lambda e^{-\mu x^{-\zeta}} \right\} = 0$$

2.3. Moments, Central Moments and Certain Related Measures

Moments can be used to investigate the model’s central tendency, skewness, dispersion, and kurtosis. If $X \sim \text{NIGT-II}(\mu, \zeta, \lambda)$, then r -th moment $\hat{\mu}_r$ of X is

$$\hat{\mu}_r = \int_0^\infty x^r dF_x(x | \mu, \zeta, \lambda); \quad r = 1, 2, \dots, \tag{18}$$

In fact, we have

$$\hat{\mu}_r = \int_0^\infty x^r \mu \zeta x^{-\zeta-1} e^{-\mu x^{-\zeta}} \left\{ \frac{1 + (1 - e^{-\mu x^{-\zeta}}) \log \lambda}{\lambda e^{-\mu x^{-\zeta}}} \right\} dx; \quad r = 1, 2, \dots, \tag{19}$$

Let $\mu x^{-\zeta} = z$, then $-\mu \zeta x^{-\zeta-1} dx = dz$, and employing series expression $\alpha^{-\rho} = \sum_{k=0}^\infty \frac{(-1)^k (\log \alpha)^k}{k!} (\rho)^k$ in (19). The final form of $\hat{\mu}_r$ is as given, as a result of simple computations on the last expression.

$$\begin{aligned} \hat{\mu}_r &= \sum_{l=0}^\infty \frac{(-1)^l (\log \lambda)^l \mu^{\frac{r}{\zeta}}}{l!} \left\{ \frac{\Gamma\left(1 - \frac{r}{\zeta}\right)}{(1+l)^{1-\frac{r}{\zeta}}} \right. \\ &\quad \left. + \Gamma\left(1 - \frac{r}{\zeta}\right) \log \lambda \left(\frac{1}{(1+l)^{1-\frac{r}{\zeta}}} - \frac{1}{(2+l)^{1-\frac{r}{\zeta}}} \right) \right\}; \quad r < \zeta. \end{aligned} \tag{20}$$

The moment formula (20) can assist users in generating useful statistical indicators. In (20), for instance, the mean (μ^*) of X gives with $r = 1$. The negative moment of X can be easily calculated by replacing r with $-\tau$ in (18).

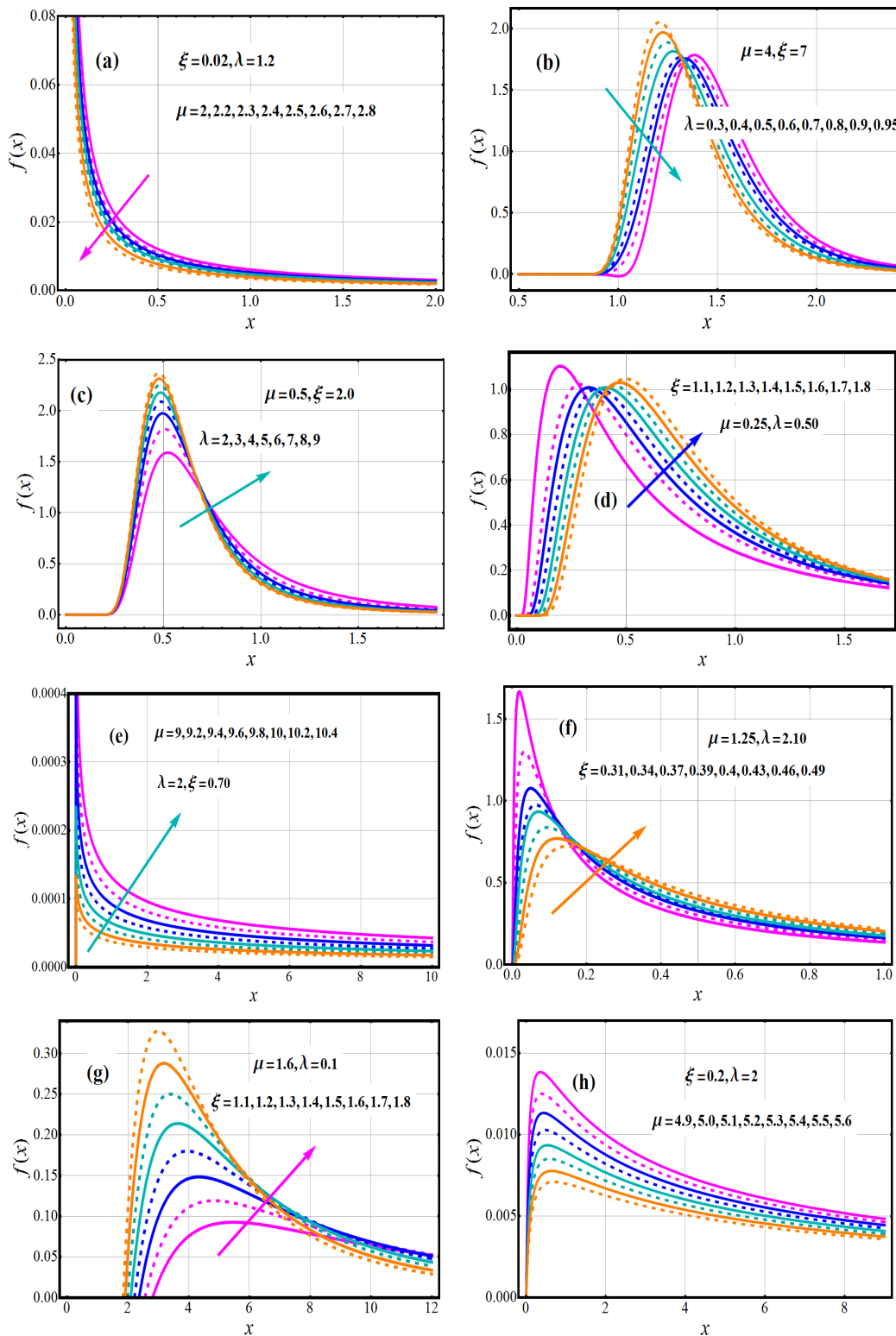


Figure 1. The performance of the PDF profile of NIGT-II model against the μ , ξ and λ (a–h).

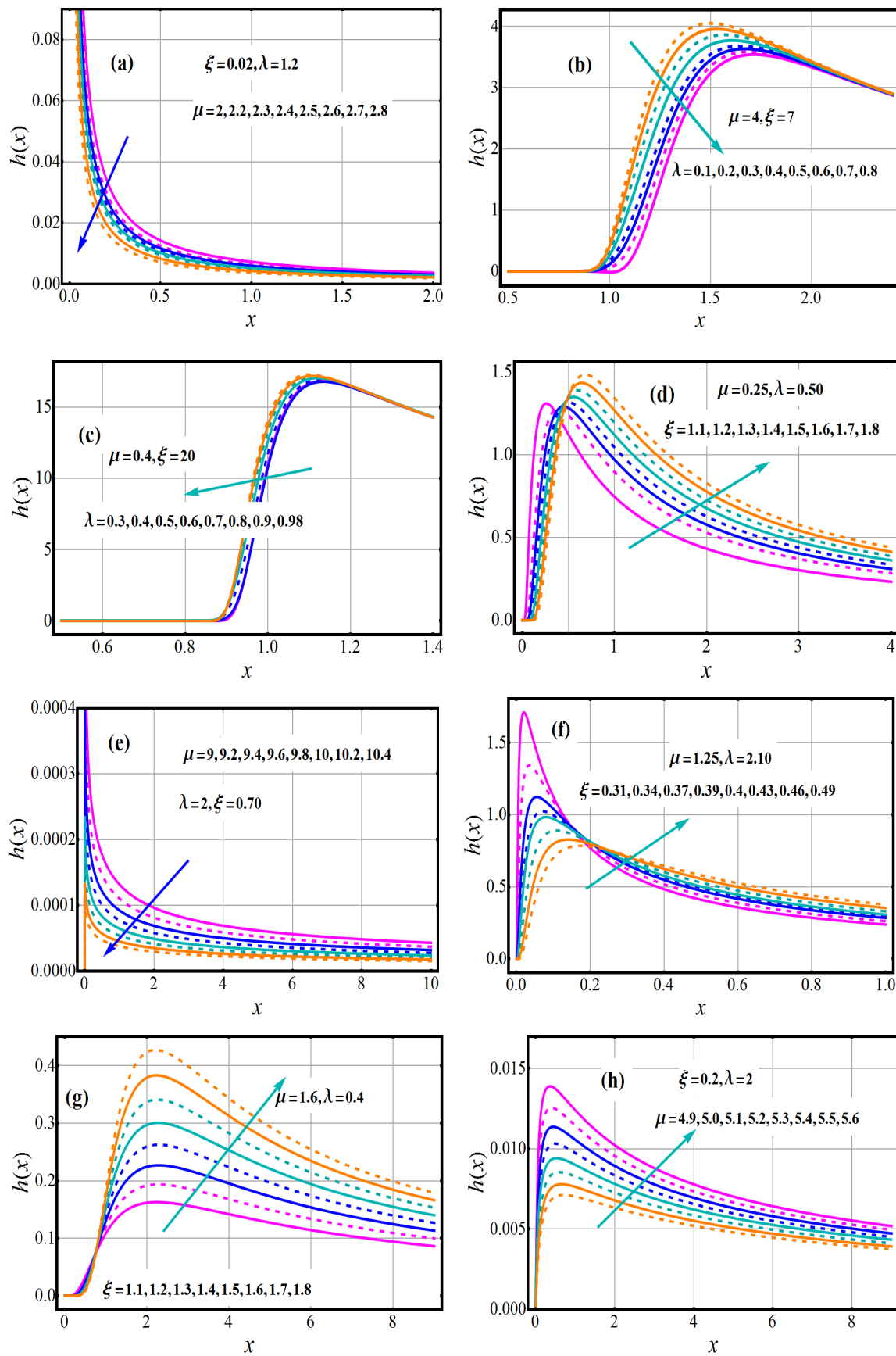


Figure 2. The performance of the FRF profile of NIGT-II model against the μ , ξ and λ (a–h).

In model assessment, the MGF is frequently used. The MGF of the NIGT-II model is

$$M_X(t|\mu, \zeta, \lambda) = E(e^{tx}) = \sum_{r=0}^{+\infty} \frac{t^r}{r!} \check{\mu}_r(\mu, \zeta, \lambda), \tag{21}$$

$$M_X(t|\mu, \zeta, \lambda) = \sum_{r=0}^{+\infty} \sum_{l=0}^{+\infty} \frac{t^r}{r!} \frac{(-1)^l (\log \lambda)^l \mu^{\frac{r}{\zeta}}}{l!} \left\{ \frac{\Gamma\left(1 - \frac{r}{\zeta}\right)}{(1+l)^{1-\frac{r}{\zeta}}} + \Gamma\left(1 - \frac{r}{\zeta}\right) \log \lambda \left(\frac{1}{(1+l)^{1-\frac{r}{\zeta}}} - \frac{1}{(2+l)^{1-\frac{r}{\zeta}}} \right) \right\}. \tag{22}$$

The central moments of the NIGT-II model are:

$$\check{\mu}_k = E(X - \mu^*)^k = \sum_{r=0}^k \binom{k}{r} \check{\mu}_r (-\mu^*)^{k-r}, \tag{23}$$

$$\check{\mu}_k = \sum_{r=0}^k \sum_{l=0}^{+\infty} \binom{k}{r} \frac{(-1)^l (\log \lambda)^l \mu^{\frac{r}{\zeta}}}{l!} (-\mu^*)^{k-r} \left\{ \frac{\Gamma\left(1 - \frac{r}{\zeta}\right)}{(1+l)^{1-\frac{r}{\zeta}}} + \Gamma\left(1 - \frac{r}{\zeta}\right) \log \lambda \left(\frac{1}{(1+l)^{1-\frac{r}{\zeta}}} - \frac{1}{(2+l)^{1-\frac{r}{\zeta}}} \right); r < \zeta \right\}. \tag{24}$$

The characteristic function for the NIGT-II model is evaluated as

$$C(t|\mu, \zeta, \lambda) = E(e^{itx}) = \int_0^{\infty} e^{itx} dF(x|\mu, \zeta, \lambda), \tag{25}$$

and using exponential series, we have

$$C(t|\mu, \zeta, \lambda) = \sum_{r=0}^{+\infty} \frac{(it)^r}{r!} \int_0^{\infty} x^r dF(x|\mu, \zeta, \lambda), \tag{26}$$

As a result, we get

$$C(t|\mu, \zeta, \lambda) = \sum_{r=0}^{+\infty} \sum_{l=0}^{\infty} \frac{(it)^r (-1)^l (\log \lambda)^l \mu^{\frac{r}{\zeta}}}{r! l!} \frac{\Gamma\left(1 - \frac{r}{\zeta}\right)}{(1+l)^{1-\frac{r}{\zeta}}} + \Gamma\left(1 - \frac{r}{\zeta}\right) \log \lambda \left(\frac{1}{(1+l)^{1-\frac{r}{\zeta}}} - \frac{1}{(2+l)^{1-\frac{r}{\zeta}}} \right); r < \zeta. \tag{27}$$

where $i = \sqrt{-1}$.

The factorial generating function of NIGT-II model is

$$F(tx|\mu, \zeta, \lambda) = \int_0^{\infty} e^{\log(1+t)x} dF(x|\mu, \zeta, \lambda), \tag{28}$$

$$F(tx|\mu, \zeta, \lambda) = \sum_{r=0}^{+\infty} \frac{\{\log(1+t)\}^r}{r!} \int_0^{\infty} x^r dF(x|\mu, \zeta, \lambda). \tag{29}$$

So we can compose the integral in (29) as

$$F(tx|\mu, \zeta, \lambda) = \sum_{r=0}^{+\infty} \sum_{l=0}^{\infty} \frac{(-1)^l (\log \lambda)^l \mu^{\frac{r}{\zeta}} \{\log(1+t)\}^r}{r!!} \times \left\{ \frac{\Gamma\left(1 - \frac{r}{\zeta}\right)}{(1+l)^{1-\frac{r}{\zeta}}} + \Gamma\left(1 - \frac{r}{\zeta}\right) \log \lambda \left(\frac{1}{(1+l)^{1-\frac{r}{\zeta}}} - \frac{1}{(2+l)^{1-\frac{r}{\zeta}}} \right) \right\}. \tag{30}$$

The mean deviation between the mean and the median, respectively, is determined by

$$\Psi_1^*(X) = \int_0^{\infty} |x - \mu^*| f(x) dx \text{ and } \Psi_2^*(X) = \int_0^{\infty} |x - \delta| f(x) dx, \tag{31}$$

where $\mu^* = E(X)$ and $\delta = \tilde{X}$. These metrics can be derived from the relationship that exists.

$$E\{|x - \vartheta|\} = \int_0^{\vartheta} (\vartheta - x) f(x) dx + \int_{\vartheta}^{\infty} (x - \vartheta) f(x) dx = 2 \int_0^{\vartheta} (\vartheta - x) f(x) dx, \tag{32}$$

$$E\{|x - \vartheta|\} = 2 \left\{ \vartheta F(\vartheta) - \int_0^{\vartheta} x f(x) dx \right\}. \tag{33}$$

After some mathematics, (33) produce the given expressions for the NIGT-II model:

$$\Psi_1^*(X) = 2 \left[\mu^* F(\mu^*) - \sum_{l=0}^{\infty} \frac{(-1)^l (\log \lambda)^l \mu^{\frac{1}{\zeta}}}{l!} \left\{ \frac{(1 + \log \lambda)}{(1+l)^{1-\frac{1}{\zeta}}} \Gamma \left\{ 1 - \frac{1}{\zeta}, (1+l)\mu / (\mu^*)^{\zeta} \right\} - \frac{\log \lambda}{(2+l)^{1-\frac{1}{\zeta}}} \Gamma \left\{ 1 - \frac{1}{\zeta}, (2+l)\mu / (\mu^*)^{\zeta} \right\} \right\} \right], \tag{34}$$

$$\Psi_2^*(X) = 2 \left[\delta F(\delta) - \sum_{l=0}^{\infty} \frac{(-1)^l (\log \lambda)^l \mu^{\frac{1}{\zeta}}}{l!} \left\{ \frac{(1 + \log \lambda)}{(1+l)^{1-\frac{1}{\zeta}}} \Gamma \left\{ 1 - \frac{1}{\zeta}, (1+l)\mu / (\delta)^{\zeta} \right\} - \frac{\log \lambda}{(2+l)^{1-\frac{1}{\zeta}}} \Gamma \left\{ 1 - \frac{1}{\zeta}, (2+l)\mu / (\delta)^{\zeta} \right\} \right\} \right], \tag{35}$$

where $F(\cdot)$ is given in (8).

3. The Estimation Technique with Simulation

Several parameter evaluation approaches have been established in research, but the maximum likelihood method is the most extensively engaged. As a result, we only evaluate the maximum likelihood estimation of NIGT-II's unknown parameters from complete samples. Simulation experiments are used to explore the effectiveness of the MLE technique. Let X_1, X_2, \dots, X_n be a random sample and related observed values, x_1, x_2, \dots, x_n from the NIGT-II model with parameter vector (μ, ζ, λ) . Then, the joint function $L(\mathbf{x} | \mu, \zeta, \lambda) = \prod_{i=1}^n f(x_i | \mu, \zeta, \lambda)$ of X_1, X_2, \dots, X_n as a log-likelihood function is

$$l(\mathbf{x} | \mu, \zeta, \lambda) = \log \prod_{i=1}^n f_{\text{NIGT-II}}(x_i | \mu, \zeta, \lambda), \tag{36}$$

$$= n \log(\mu) + n \log(\zeta) - (\zeta + 1) \sum_{i=1}^n \log(x_i) - \mu \sum_{i=1}^n x_i^{-\zeta} + \sum_{i=1}^n \log\left(1 + \left(1 - e^{-\mu x_i^{-\zeta}}\right) \log \lambda\right) - e^{-\mu \sum_{i=1}^n x_i^{-\zeta}} \log(\lambda), \tag{37}$$

$$\frac{\partial l(\mathbf{x} | \mu, \zeta, \lambda)}{\partial \mu} = \frac{n}{\mu} + \sum_{i=1}^n x_i^{-\zeta} \left\{ \log(\lambda) e^{-\mu \sum_{i=1}^n x_i^{-\zeta}} - 1 \right\} + \log \lambda \sum_{i=1}^n \frac{x_i^{-\zeta} e^{-\mu x_i^{-\zeta}}}{1 + \left(1 - e^{-\mu x_i^{-\zeta}}\right) \log \lambda}, \tag{38}$$

$$\begin{aligned} \frac{\partial l(\mathbf{x} | \mu, \zeta, \lambda)}{\partial \zeta} &= \frac{n}{\zeta} - \sum_{i=1}^n \log(x_i) - \mu \left\{ \log(\lambda) e^{-\mu \sum_{i=1}^n x_i^{-\zeta}} - 1 \right\} \sum_{i=1}^n \log(x_i) x_i^{-\zeta} \\ &\quad - \mu \log \lambda \sum_{i=1}^n \frac{\log(x_i) x_i^{-\zeta} e^{-\mu x_i^{-\zeta}}}{1 + \left(1 - e^{-\mu x_i^{-\zeta}}\right) \log \lambda}, \end{aligned} \tag{39}$$

$$\frac{\partial l(\mathbf{x} | \mu, \zeta, \lambda)}{\partial \lambda} = -\frac{e^{-\mu \sum_{i=1}^n x_i^{-\zeta}}}{\lambda} + \sum_{i=1}^n \frac{1 - e^{-\mu x_i^{-\zeta}}}{\lambda \left\{ 1 + \left(1 - e^{-\mu x_i^{-\zeta}}\right) \log \lambda \right\}}. \tag{40}$$

The MLEs of the parameters are provided by simultaneously solving (38)–(40). According to the simulation study, the bias and mean square error (MSEs) of MLEs reduce as n increases, with a few exceptions, which fulfills the standard requirements of the asymptotic features of MLEs. In particular, all parameter combinations that approach zero show fluctuation in bias and MSEs. Such reflections can be found in Tables 1–3. One of the most important features of the likelihood function for any probability density is that the parameter estimates obtained by MLEs must be maximum in order to ensure that such a problem is addressed. We plot the $l(\mathbf{x} | \mu, \zeta, \lambda)$ (as shown in next section). The assessments obtained from MLEs for specified parameters are the global maximum instead of the local maximum for all parameters, as shown in next section.

Table 1. Numerical outcomes of AB and MSE values of the NIGT-II model for $\mu = 2.7, \zeta = 3.9, \lambda = 1.5$.

n	30	60	90	120	150	200	250	300
AB ($\hat{\mu}$)	−0.6798	−1.4745	−0.9406	−0.5781	−0.2624	−0.0906	−0.0126	−0.0022
MSE ($\hat{\mu}$)	14.0628	7.5942	3.3225	1.6586	0.6990	0.1447	0.0372	0.0102
RMSE ($\hat{\mu}$)	3.7500	2.7556	1.8228	1.2879	0.8361	0.3804	0.1929	0.1010
AB ($\hat{\zeta}$)	−1.3447	−0.4420	−0.2082	0.0037	−0.0747	−0.1310	−0.0120	−0.0057
MSE ($\hat{\zeta}$)	19.7444	7.0729	3.6850	0.8708	0.4919	0.0947	0.0186	0.0056
RMSE ($\hat{\zeta}$)	4.4435	2.6595	1.9196	0.9332	0.7014	0.3077	0.1364	0.0748
AB ($\hat{\lambda}$)	3.7467	2.6824	1.7273	1.1094	0.8106	0.5185	0.4254	0.4007
MSE ($\hat{\lambda}$)	19.5671	9.4809	4.0358	1.7487	1.0418	0.3618	0.2078	0.1691
RMSE ($\hat{\lambda}$)	4.4235	3.0791	2.0089	1.3224	1.0207	0.6015	0.4559	0.4112

Table 2. Numerical outcomes of AB and MSE values of the NIGT-II model for $\mu = 6.2, \zeta = 4.7, \lambda = 2.5$.

<i>n</i>	30	60	90	120	150	200	250	300
AB ($\hat{\mu}$)	−3.2225	−2.6637	−1.9319	−1.0792	−0.4402	−0.1559	−0.0473	0.0067
MSE ($\hat{\mu}$)	31.3787	20.3257	10.9748	4.9336	2.4360	0.6238	0.1439	0.0296
RMSE ($\hat{\mu}$)	5.6017	4.5084	3.3128	2.2211	1.5608	0.7898	0.3793	0.1721
AB ($\hat{\zeta}$)	−0.0100	0.1000	0.4813	0.3048	−0.0298	−0.0034	0.0158	−0.0303
MSE ($\hat{\zeta}$)	38.6967	16.7172	8.2162	4.2350	2.8566	1.0083	0.2097	0.0833
RMSE ($\hat{\zeta}$)	6.2207	4.0887	2.8664	2.0579	1.6902	1.0041	0.4579	0.2886
AB ($\hat{\lambda}$)	5.2271	3.8114	2.7165	1.9901	1.4649	0.9112	0.7099	0.6502
MSE ($\hat{\lambda}$)	30.2567	8.7565	6.0339	3.7317	2.0582	1.1490	0.5851	0.4626
RMSE ($\hat{\lambda}$)	5.5006	2.9591	2.4564	1.9318	1.4346	1.0719	0.7649	0.6802

Table 3. Numerical outcomes of AB and MSE values of the NIGT-II model for $\mu = 1.9, \zeta = 3.3, \lambda = 4.5$.

<i>n</i>	30	60	90	120	150	200	250	300
AB ($\hat{\mu}$)	3.5950	2.3918	0.8990	0.4357	0.3729	0.3730	0.3870	0.3678
MSE ($\hat{\mu}$)	28.4725	10.6806	1.6142	0.3166	0.1745	0.1679	0.0622	0.0100
RMSE ($\hat{\mu}$)	5.3360	3.2681	1.2705	0.5627	0.4177	0.4098	0.2494	0.1000
AB ($\hat{\zeta}$)	−1.7791	−2.2027	−0.9700	−0.2214	−0.0300	0.0009	0.0005	0.0000
MSE ($\hat{\zeta}$)	17.9104	11.8278	2.6780	0.4129	0.0384	0.0016	0.0000	0.0000
RMSE ($\hat{\zeta}$)	4.2321	3.4392	1.6365	0.6426	0.1960	0.0400	0.0000	0.0000
AB ($\hat{\lambda}$)	1.2342	1.0209	0.5318	0.1844	0.0934	0.0779	0.0630	0.0522
MSE ($\hat{\lambda}$)	4.3975	2.0200	0.6003	0.1300	0.0428	0.0382	0.0289	0.0235
RMSE ($\hat{\lambda}$)	2.0970	1.4213	0.7748	0.3606	0.2069	0.1955	0.1700	0.1533

4. Numerical and Graphical Analysis

The NIGT-II model’s MaxLLE estimators are not in closed form, as stated in the previous section. As a consequence, a simulation experiment is run to evaluate the performance of estimates using different metrics including MSEs, RMSE, and average bias (AB) values, as well as their asymptotic performance for finite samples. We can use numerical and graphical simulation studies to examine the finite sample behavior of MLEs. The given algorithm was used to make the decision:

1. Generate a thousand samples of size *n* from (9). QF accomplished all of the work and gleaned the data from a uniform model.
2. The exact values of various combinations of μ, ζ and λ are taken into account as set-I: (2.7, 3.9, 1.5), set-II: (6.2, 4.7, 2.5), and set-III: (1.9, 3.3, 4.5). The theoretical and simulated density functions of the NIGT-II distribution for these choices are shown in Figure 3.
3. Evaluate the estimates for 1000 samples, say $(\check{\mu}_k, \check{\zeta}_k, \check{\lambda}_k)$ for $k = 1, 2, \dots, 1000$.
4. Examine the AB value, as well as the MSEs and RMSEs. The following formulas are used to find these targets:

$$AB_{\Psi}(n) = \frac{1}{1000} \sum_{i=1}^{1000} (\check{\Psi}_i - \Psi), \tag{41}$$

$$MSE_{\Psi}(n) = \frac{1}{1000} \sum_{i=1}^{1000} (\check{\Psi}_i - \Psi)^2, \tag{42}$$

$$RMSE_{\Psi}(n) = \sqrt{\frac{1}{1000} \sum_{i=1}^{1000} (\check{\Psi}_i - \Psi)^2}. \tag{43}$$

where $\Psi = (\mu, \xi, \lambda)$.

5. These steps have been repeated with specified parameters for MLEs for $n = 30, 40, \dots, 300$. The bias $\psi(n)$ and MSE $\psi(n)$ have both been evaluated. To assess the quality of the estimations, we implemented R's optim function. The findings of the experiments are shown in Tables 1–3 and Figures 4–6. In Figures 4–6, the ABs and MSEs vary w.r.t. n .

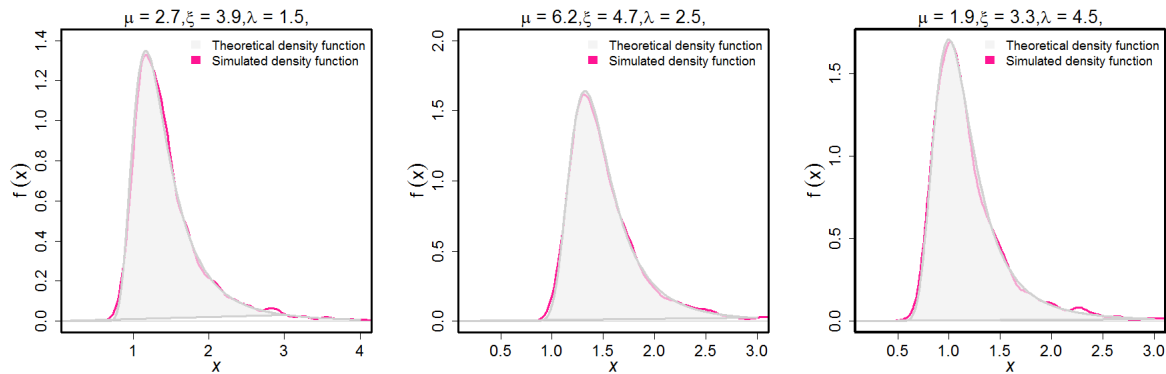


Figure 3. Simulated model for a parametric set I to III.

The bias gradually decreases until it reaches zero as n rises, we thus conclude that estimators have an asymptotic unbiasedness property. The MSE trend, on the other hand, implies consistency as the error approaches zero as n increases.

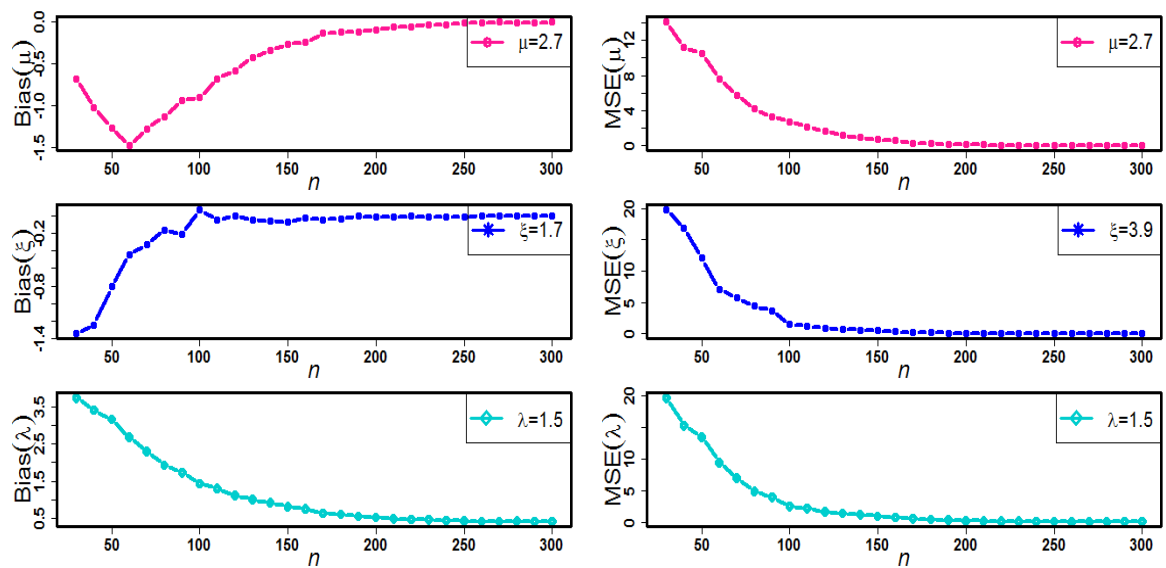


Figure 4. The performance of Bias and MSE profiles against $\check{\mu}$, $\check{\xi}$ and $\check{\lambda}$ for set-I.

As mentioned in the discussion, the study's findings are explained through figures and tables. The following are the key conclusions of the investigation:

- Tables 1–3 indicate the RMSE, MSE and AB values of parameters for various n , and it can be shown that MSE and RMSE decrease with increasing n , as intended. Secondly, as n rises, the AB decreases.
- As n increases, the biases of $\check{\mu}$, $\check{\lambda}$ and $\check{\xi}$ diminish.
- Although the biases of $\check{\mu}$ and $\check{\xi}$ are predominantly negative, there are positive biases for $\check{\lambda}$.
- The MLEs of $\check{\mu}$ and $\check{\xi}$ are overvalued, whereas the MLEs of $\check{\lambda}$ are undervalued (see Figures 4–6 (left panel)).

- The MaxLLE technique outperforms in terms of MSE, as seen in the right panel of Figures 4–6.
- When n rises, all bias and MSE figures for $\check{\mu}$, $\check{\lambda}$ and $\check{\xi}$ ultimately approach zero, as seen in Figures 4–6. This highlights the precision of estimating procedures.
- In comparison to the MSE of $\check{\xi}$, the MSE of $\check{\mu}$ and $\check{\lambda}$ is quite small.
- Depending on these findings, we conclude that MLEs perform a reasonable job of estimating parameters and that values for these sample sizes appear to be reasonably stable and close to exact values. This information shows that MLEs are both efficient and consistent.

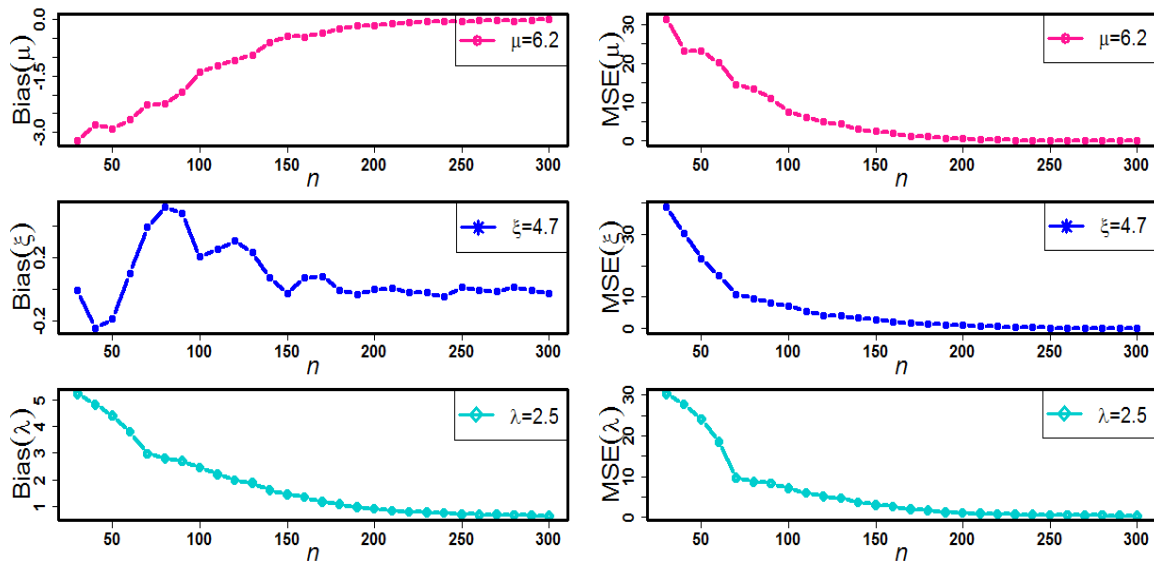


Figure 5. The performance of bias and MSE profiles against $\check{\mu}$, $\check{\xi}$ and $\check{\lambda}$ for set-II.

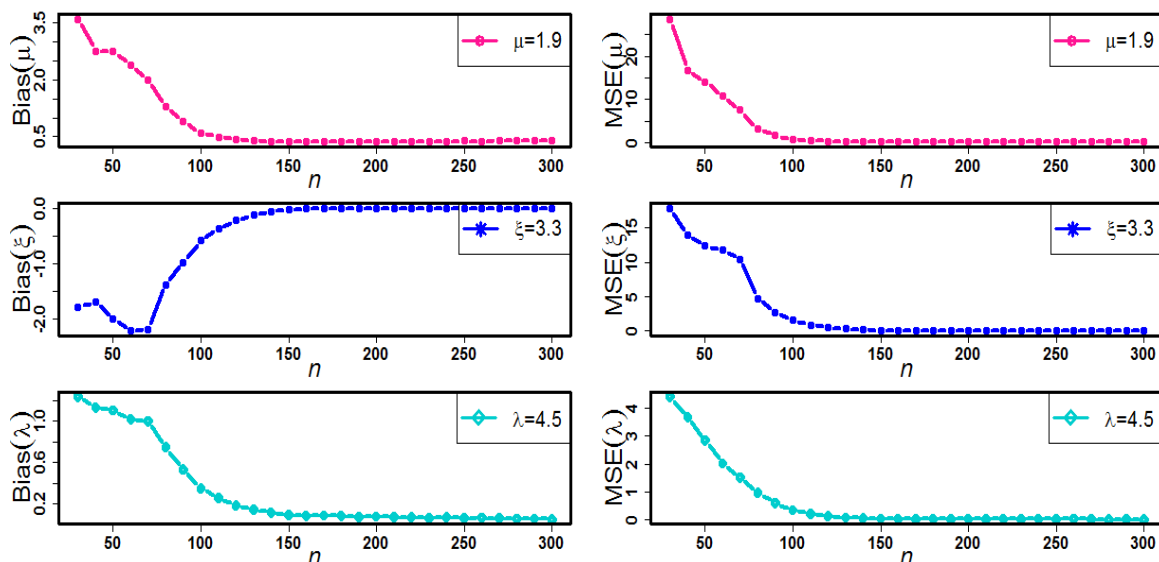


Figure 6. The performance of bias and MSE profiles against $\check{\mu}$, $\check{\xi}$ and $\check{\lambda}$ for set-III.

5. Illustrative Examples

The utility of the NIGT-II model for real data sets is given here. Alternatives to the NIGT-II model include the Gumbel Type-Two (GT-II) distribution. These models were compared via goodness of fit (GOF) measures such as Bayesian information criterion (BIC), Akaike information criterion (AIC), corrected Akaike information criterion (CAIC) and negative log-likelihood (NLL). The model with the smallest analytical metrics scores for

real data sets may be the perfect suited. The findings of such investigations are presented in Tables 4 and 5. COVID-19 data from the United Kingdom was presented in the first real data collection, which spanned 82 days from May 1 to July 16, 2021, and COVID-19 data from France was presented in the second real data collection, which spanned 108 days from March 1 to June 16, 2021; both were made available at <https://covid19.who.int/> (accessed on 3 March 2022) . Abu El Azm et al. [46] provides more information on these datasets. Other COVID-19 data applications can be found in [47,48]. The MaxLLE technique has been implemented to examine the relevant parameters of models. For two real data sets, Tables 4 and 5 show MLEs and associated standard errors (SEs) in parenthesis. The findings in these tables show that the proposed model fits better than the benchmark model since the NIGT-II model has the smallest analytical measures. Figures 7 and 8 illustrate the P-P patterns of the NIGT-II distribution for the two real data sets, respectively. These numbers back up the findings in Tables 4 and 5 that the NIGT-II model fits the two real data sets well. For the two real data sets, Figures 9 and 10 show profile-likelihood graphs of the NIGT-II parameters. For all estimated parameters, these plots demonstrate the unimodality of profile-likelihood functions. Finally, for both datasets, the NIGT-II model appears as the best adequate model, demonstrating its use in a practical setting.

Table 4. Statistical outcomes of NIGT-II and GT-II models for the first data.

Models	MLEs	NLL	AIC	BIC	AICC
NIGT-II ($\check{\mu}, \check{\zeta}, \check{\lambda}$)	0.003704, 1.186428, 0.434443 0.001621, 0.089687, 0.047923	−186.8589	−367.7178	−360.4976	−367.4101
GT-II ($\check{\theta}, \check{\kappa}$)	0.014746, 1.016119 0.005563, 0.077277	−182.5156	−361.0312	−356.2178	−360.8793

Table 5. Statistical outcomes of NIGT-II and GT-II models for the second data.

Models	MLEs	NLL	AIC	BIC	AICC
NIGT-II ($\check{\mu}, \check{\zeta}, \check{\lambda}$)	0.007352, 1.126818, 0.426782 0.002354, 0.069947, 0.034165	−201.7573	−397.5145	−389.4682	−397.2838
GT-II ($\check{\theta}, \check{\kappa}$)	0.028103, 0.952045 0.007874, 0.060660	−193.8848	−383.7696	−378.4053	−383.6553

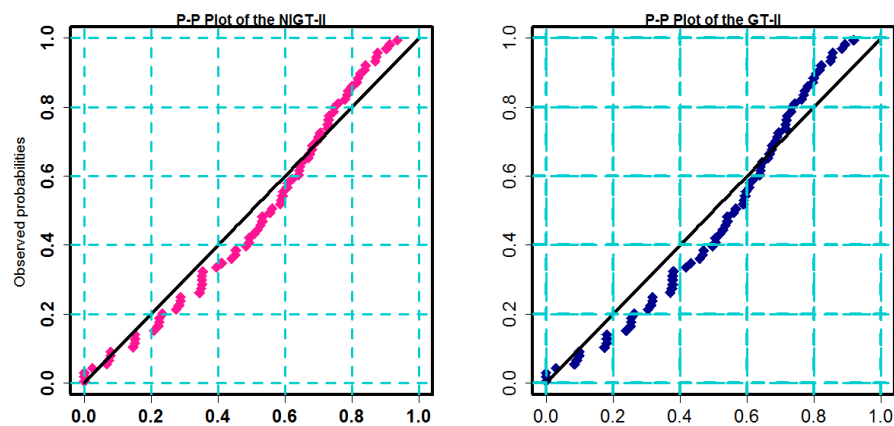


Figure 7. Probability plots of NIGT-II and GT-II models for dataset I.

Closing remarks on both applications

1. NIGT-II has the lowest values of analytical measures of GOF statistics, in accordance with both datasets.

2. As seen in Figures 7 and 8, NIGT-II is the most effective model for fitting datasets I and II.
3. The GT-II distribution demonstrates a poor fit for both datasets, as shown in Tables 4 and 5.
4. Figures 9 and 10 indicated the existence of estimated parameters for the proposed model for the two real data sets, respectively.
5. The log-likelihood function has a global maximum root for the model parameters, as shown in Figures 9 and 10.

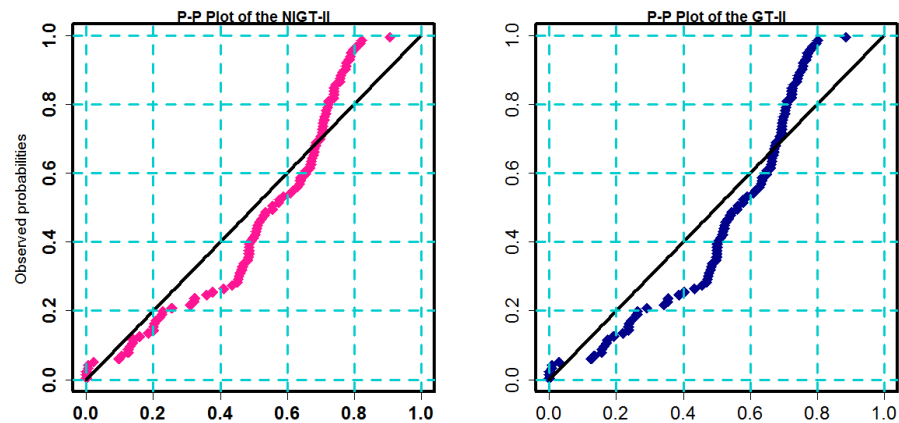


Figure 8. Probability plots of NIGT-II and GT-II models for dataset II.

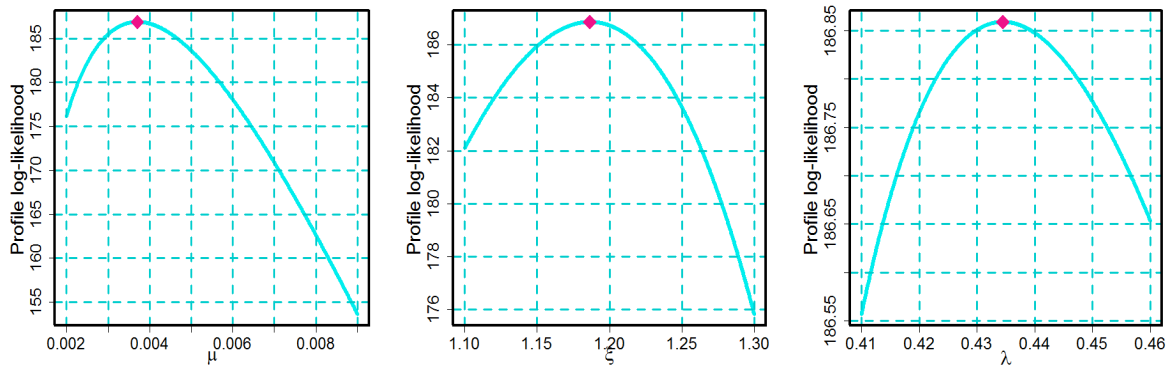


Figure 9. Curves of the profile-likelihood function of three estimated parameters of NIGT-II model for the first real data set.

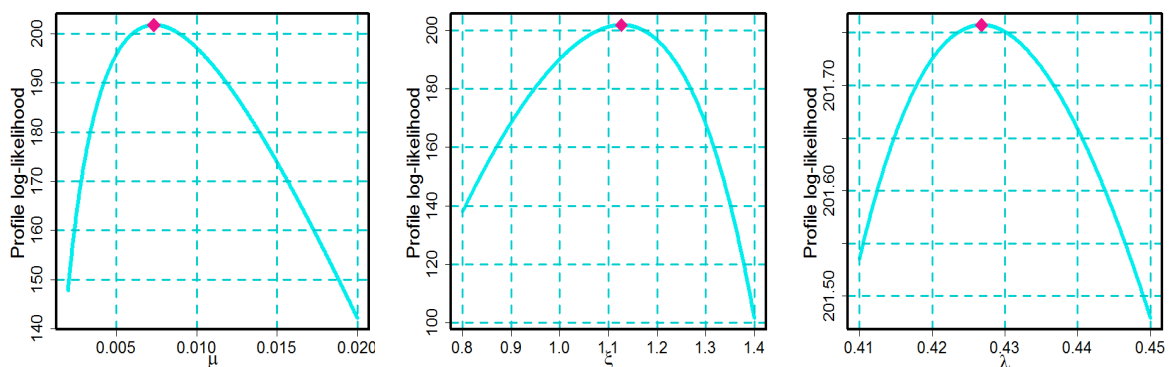


Figure 10. Curves of the profile-likelihood function of three estimated parameters of NIGT-II model for the second real data set.

6. Concluding Remarks

This work proposes a three-parameter model for the new and improved Gumbel Type-II (NIGT-II). The NIGT-II model is more versatile than the benchmark model when it comes to interpreting lifespan data. This is a quick overview of what we are attempting to achieve. Estimation techniques such as MaxLLE are used to assess the parameters of the NIGT-II model. A simulation experiment is performed to evaluate the model's execution over a range of sample sizes and parameter values. Depending on the COVID-19 mortality rate, we consider two accomplishments. We determined that it outperformed its competitor in terms of analytical results, making it the ideal selection. We also graphed Figures 9 and 10 for the profile-likelihood function of the given model with its parameters for the real data sets to ensure that the roots of the proposed model's MLE offer a maximum value. These graphs show that the profile-likelihood functions of all estimated parameters are unimodal. Further research will include validating this model utilizing other recent data sets. A new two-parameter model using the Kavya–Manoharan (KM) transformation will also be included in future studies, as well as other estimating techniques to evaluate the effectiveness of the NIGT-II distribution parameters.

Author Contributions: Conceptualization, S.A.L., T.N.S., M.K.H.H., T.A.A., S.A. and A.S.; Methodology, S.A.L., T.N.S., M.K.H.H., T.A.A., S.A. and A.S.; Software, T.N.S. and A.S.; Formal analysis, S.A.L., T.N.S., M.K.H.H. and S.A.; Investigation, S.A.L., T.N.S., M.K.H.H. and A.S.; Resources, T.A.A.; Data curation, S.A.L., T.N.S. and T.A.A.; Writing—original draft, S.A.L., T.N.S., M.K.H.H., T.A.A. and S.A.; Writing—review & editing, T.N.S. and A.S.; Visualization, T.N.S.; Supervision, T.A.A. and A.S.; Funding acquisition, T.A.A. All authors have read and agreed to the published version of the manuscript.

Funding: The authors would like to thank the Deanship of Scientific Research at Umm Al-Qura University for supporting this work by Grant Code 22UQU4310063DSR14.

Data Availability Statement: All data generated or analyzed during this study are included in this article.

Conflicts of Interest: The authors declare no conflict of interest.

Nomenclature

Symbols

$f(x .)$	PDF
$F(x .)$	CDF
$S(x .)$	SF/RF
$h(x .)$	HRF/FRF
$H(x .)$	CHRF
$F(tx .)$	FGF
$C(t .)$	Cumulants
$M(t .)$	MGF
δ	Median
$\tilde{\mu}_k$	Central Moments
$\Psi_1^*(X)$	Mean deviation about mean
$\Psi_2^*(X)$	Mean deviation about median

Abbreviations

MaxLLE	Maximum likelihood Estimation
FGF	Factorial Generating Function
GT-II	Gumbel Type-II
RMSE	Root Mean Square Error
PDF	Probability Density Function
CDF	Cumulative Distribution Function

MLEs	Maximum likelihood Estimates
MN	Monotonic
SF	Survival Function
FRF	Failure Rate Function
HRF	Hazard Rate Function
CHRF	Cumulative Hazard Rate Function
AB	Average Bias
NMNHf	Non-Monotonic Hazard Function
w.r.t.	With Respect To
QF	Quantile Function
MGF	Moment Generating Function
r.v.	Random Variable
MSE	Mean Square Error

References

- Gupta, R.C. Nonmonotonic failure rates and mean residual life functions. In *System Furthermore, Bayesian Reliability: Essays in Honor of Professor Richard E Barlow on His 70th Birthday*; World Scientific Publishing Co.: River Edge, NJ, USA, 2001; pp. 147–163.
- Deshpande, J.V.; Suresh, R.P. Non-monotonic ageing. *Scand. J. Stat.* **1990**, *17*, 257–262.
- Weibull, W. A statistical distribution function of wide applicability. *J. Appl. Mech.* **1951**, *18*, 293–297. [[CrossRef](#)]
- Eugene, N.; Lee, C.; Famoye, F. Beta-normal distribution and its applications. *Commun.-Stat.-Theory Methods* **2002**, *31*, 497–512. [[CrossRef](#)]
- Jones, M.C. Families of distributions arising from distributions of order statistics. *Test* **2004**, *13*, 1–43. [[CrossRef](#)]
- Cordeiro, G.M.; de Castro, M. A new family of generalized distributions. *J. Stat. Comput. Simul.* **2011**, *81*, 883–898. [[CrossRef](#)]
- Alexander, C.; Cordeiro, G.M.; Ortega, E.M.; Sarabia, J.M. Generalized beta-generated distributions. *Comput. Stat. Data Anal.* **2012**, *56*, 1880–1897. [[CrossRef](#)]
- Cordeiro, G.M.; Ortega, E.M.; da Cunha, D.C. The exponentiated generalized class of distributions. *J. Data Sci.* **2013**, *11*, 1–27. [[CrossRef](#)]
- Ristić, M.M.; Balakrishnan, N. The gamma-exponentiated exponential distribution. *J. Stat. Simul.* **2012**, *82*, 1191–1206. [[CrossRef](#)]
- Cordeiro, G.M.; Ortega, E.M.; Popović, B.V.; Pescim, R.R. The Lomax generator of distributions: Properties, minification process and regression model. *Appl. Math. Comput.* **2014**, *247*, 465–486. [[CrossRef](#)]
- Tahir, M.H.; Cordeiro, G.M.; Alzaatreh, A.; Mansoor, M; Zubair, M. The logistic-X family of distributions and its applications. *Commun.-Stat.-Theory Methods* **2016**, *45*, 7326–7349. [[CrossRef](#)]
- Tahir, M.H.; Zubair, M.; Mansoor, M.; Cordeiro, G.M.; Alizadeh, M.; Hamedani, G.G. A new Weibull-G family of distributions. *Hacet. J. Math. Stat.* **2016**, *45*, 629–647. [[CrossRef](#)]
- Tahir, M.H.; Cordeiro, G.M.; Alizadeh, M.; Mansoor, M.; Zubair, M.; Hamedani, G.G. The odd generalized exponential family of distributions with applications. *J. Stat. Distrib. Appl.* **2015**, *2*, 1–28. [[CrossRef](#)]
- Zografos, K.; Balakrishnan, N. On families of beta- and generalized gamma generated distributions and associated inference. *Stat. Methodol.* **2009**, *6*, 344–362. [[CrossRef](#)]
- Reyad, H.; Korkmaz, M. Ç.; Afify, A.Z.; Hamedani, G. G.; Othman, S. The Fréchet Topp Leone-G family of distributions: Properties, characterizations and applications. *Ann. Data Sci.* **2021**, *8*, 345–366. [[CrossRef](#)]
- Aldeni, M.; Lee, C.; Famoye, F. Families of distributions arising from the quantile of generalized lambda distribution. *J. Stat. Distrib. Appl.* **2017**, *4*, 1–18. [[CrossRef](#)]
- Alzaatreh, A.; Lee, C.; Famoye, F. T-normal family of distributions: A new approach to generalize the normal distribution. *J. Stat. Distrib. Appl.* **2014**, *1*, 1–18. [[CrossRef](#)]
- Cordeiro, G.M.; Alizadeh, M.; Ramires, T.G.; Ortega, E.M. The generalized odd half-Cauchy family of distributions: Properties and applications. *Commun.-Stat.-Theory Methods* **2017**, *46*, 5685–5705. [[CrossRef](#)]
- Jones, M.C. Kumaraswamy's distribution: A beta-type distribution with some tractability advantages. *Stat. Methodol.* **2009**, *6*, 70–81. [[CrossRef](#)]
- Mahdavi, A.; Kundu, D. A new method for generating distributions with an application to exponential distribution. *Commun.-Stat.-Theory Methods* **2017**, *46*, 6543–6557. [[CrossRef](#)]
- Nassar, M.; Alzaatreh, A.; Mead, M.; Abo-Kasem, O. Alpha power Weibull distribution: Properties and applications. *Commun.-Stat.-Theory Methods* **2017**, *46*, 10236–10252. [[CrossRef](#)]
- Ramadan, D.A.; Magdy, W. On the alpha-power inverse Weibull distribution. *Int. J. Comput. Appl.* **2018**, *181*, 6–12.
- Dey, S.; Alzaatreh, A.; Zhang, C.; Kumar, D. A new extension of generalized exponential distribution with application to ozone data. *Ozone Sci. Eng.* **2017**, *39*, 273–285. [[CrossRef](#)]
- Dey, S.; Nassar, M.; Kumar, D. Alpha power transformed inverse Lindley distribution: A distribution with an upside-down bathtub-shaped hazard function. *J. Comput. Applied Math.* **2019**, *348*, 130–145. [[CrossRef](#)]
- Dey, S.; Ghosh, I.; Kumar, D. Alpha-power transformed Lindley distribution: Properties and associated inference with application to earthquake data. *Ann. Data Sci.* **2019**, *6*, 623–650. [[CrossRef](#)]

26. Ijaz, M.; Asim, S.M.; Farooq, M.; Khan, S.A.; Manzoor, S. A Gull Alpha Power Weibull distribution with applications to real and simulated data. *PLoS ONE* **2020**, *15*, e0233080. [[CrossRef](#)]
27. Brito, E.; Silva, G.O.; Cordeiro, G.M.; Demétrio, C.G.B. The mcdonald gumbel model. *Commun.-Stat.-Theory Methods* **2016**, *45*, 3367–3382. [[CrossRef](#)]
28. Gupta, J.; Garg, M.; Gupta, M. The Lomax-Gumbel Distribution. *Palest. J. Math.* **2016**, *5*, 35–42.
29. Gholami, G.; Pourdarvish, A.; MirMostafae, S.M.T.; Alizadeh, M.; Nashi, A.N. On The Gamma Gumbel Distribution. *Appl. Math. E-Notes* **2020**, *20*, 142–154.
30. Nadarajah, S.; Kotz, S. The beta Gumbel distribution. *Math. Probl. Eng.* **2004**, *2004*, 323–332. [[CrossRef](#)]
31. Ogunde, A.A.; Fayose, S.T.; Ajayi, B.; Omosigho, D.O. Extended Gumbel type-2 distribution: Properties and applications. *J. Appl. Math.* **2020**, *2020*, 1–11. [[CrossRef](#)]
32. Alzaatreh, A. New Method for Generating Families of Continuous Distributions. Ph.D. Thesis, Central Michigan University, Mount Pleasant, MI, USA, 2011. Available online: <http://condor.cmich.edu/cdm/ref/collection/p1610-01coll1/id/3447> (accessed on 3 March 2022).
33. Alzaatreh, A.; Lee, C.; Famoye, F. A new method for generating families of continuous distributions. *Metron* **2013**, *71*, 63–79. [[CrossRef](#)]
34. Lone, S.A.; Sindhu, T.N.; Jarad, F. Additive Trinomial Fréchet distribution with practical application. *Results Phys.* **2022**, *33*, 105087. [[CrossRef](#)]
35. Dey, S.; Mazucheli, J.; Nadarajah, S. Kumaraswamy distribution: Different methods of estimation. *Comput. Appl. Math.* **2018**, *37*, 2094–2111. [[CrossRef](#)]
36. Sindhu, T.N.; Hussain, Z.; Aslam, M. Parameter and reliability estimation of inverted Maxwell mixture model. *J. Stat. Manag. Syst.* **2019**, *22*, 459–493. [[CrossRef](#)]
37. Kundu, D.; Raqab, M.Z. Generalized Rayleigh distribution: Different methods of estimations. *Comput. Stat. Data Anal.* **2005**, *49*, 187–200. [[CrossRef](#)]
38. Sindhu, T.N.; Aslam, M.; Shafiq, A. Bayesian analysis of two censored shifted Gompertz mixture distributions using informative and noninformative priors. *Pak. J. Stat. Oper. Res.* **2017**, 227–243. [[CrossRef](#)]
39. Sindhu, T.N.; Aslama, M.; Shafiq, A. Analysis of the Left Censored Data from the Pareto Type II Distribution. *Casp. J. Appl. Sci. Res.* **2013**, *2*, 53–62.
40. Dey, S.; Ali, S.; Park, C. Weighted exponential distribution: Properties and different methods of estimation. *J. Stat. Comput. Simul.* **2015**, *85*, 3641–3661. [[CrossRef](#)]
41. Teimouri, M.; Hoseini, S.M.; Nadarajah, S. Comparison of estimation methods for the Weibull distribution. *Statistics* **2013**, *47*, 93–109. [[CrossRef](#)]
42. Sindhu, T.N.; Khan, H.M.; Hussain, Z.; Al-Zahrani, B. Bayesian inference from the mixture of half-normal distributions under censoring. *J. Natl. Sci. Found. Sri Lanka* **2018**, *46*, 587–600. [[CrossRef](#)]
43. Sindhu, T.N.; Hussain, Z.; Aslam, M. On the Bayesian analysis of censored mixture of two Topp-Leone distribution. *Sri Lankan J. Appl. Stat.* **2019**, *19*, 13. [[CrossRef](#)]
44. Tahir, M.H.; Cordeiro, G.M.; Alzaatreh, A.; Mansoor, M.; Zubair, M. A new Weibull–Pareto distribution: Properties and applications. *Commun.-Stat.-Simul. Comput.* **2016**, *45*, 3548–3567. [[CrossRef](#)]
45. Hyndman, R.J.; Fan, Y. Sample quantiles in statistical packages. *Am. Stat.* **1996**, *50*, 361–365.
46. Abu El Azm, W.S.; Almetwally, E.M.; Naji AL-Aziz, S.; El-Bagoury, A.A.A.H.; Alharbi, R.; Abo-Kasem, O.E. A new transmuted generalized lomax distribution: Properties and applications to COVID-19 data. *Comput. Intell. Neurosci.* **2021**, *2021*, 5918511. [[CrossRef](#)] [[PubMed](#)]
47. Shafiq, A.; Sindhu, T.N.; Alotaibi, N. A novel extended model with versatile shaped failure rate: Statistical inference with COVID-19 applications. *Results Phys.* **2022**, *36*, 105–398. [[CrossRef](#)] [[PubMed](#)]
48. Sindhu, T.N.; Shafiq, A.; Al-Mdallal, Q.M. Exponentiated transformation of Gumbel Type-II distribution for modeling COVID-19 data. *Alex. Eng. J.* **2021**, *60*, 671–689. [[CrossRef](#)]

Disclaimer/Publisher’s Note: The statements, opinions and data contained in all publications are solely those of the individual author(s) and contributor(s) and not of MDPI and/or the editor(s). MDPI and/or the editor(s) disclaim responsibility for any injury to people or property resulting from any ideas, methods, instructions or products referred to in the content.